The Influence of Cooling Rate and Composition on Weld Metal Microstructures in a C/Mn and a HSLA Steel

With a C/Mn weld metal (C = 0.13%), microstructure changes from martensite to upper bainite to acicular ferrite as heat input goes from 0.74 to 10 kJ/mm, and for a HSLA weld metal (C = 0.07%) microstructure changes from ferrite to acicular ferrite to upper bainite when increasing cooling rate

BY A. G. GLOVER, J. T. McGRATH, M. J. TINKLER and G. C. WEATHERLY

ABSTRACT. A series of weldments were prepared in C/Mn and HSLA steels by the submerged arc process. The weld metal microstructure was studied as a function of heat input/cooling rate and composition.

The gross microstructure of the C/Mn Series "A" weld metals ($C \geq 0.13\%$) was found to change from martensite to upper bainite to acicular ferrite as the heat input was increased from 0.74 to 10 kJ/mm. An M-A microconstituent residing between the ferrite laths was replaced by carbides with increasing heat input (decreasing cooling rate).

For the HSLA Series "B" weld metal (C = 0.07%), increasing the cooling rate resulted in the gross microstructure changing from coarse, polygonal ferrite to acicular ferrite to upper bainite. In the cooling range, $15 < \Delta t < 190$ seconds, a blocky or elongated M-A microconstituent was observed. The absence of any distinct carbide formation in this cooling range was noted.

Introduction

The attainment of maximum weld metal fracture toughness in engineering structures of high integrity, such as large diameter gas pipelines and nuclear power station components, has been the objective of many recent welding research programs.[1-3] Specifically, it has been shown that toughness in C/Mn and high-strength low-alloy (HSLA) weldments is controlled by weld metal microstructure.[4]

Before one can control weld microstructure and, thus, the fracture properties, a thorough knowledge of the type and amounts of the various constituents is essential. This requires quantitative metallographic analysis, using both optical and transmission electron microscopy techniques.

In terms of gross microstructure, it has been shown that high fracture toughness is associated with a fine acicular ferrite structure and a low inclusion content.[5,6] Poor toughness results from a high proportion of coarse upper bainite.[7] The role of proeutectoid ferrite is less well defined but is also believed to lower toughness.[8] Although martensite is more likely to be found in significant amounts in the HAZ, it can also have a deleterious effect on weld metal toughness.

More detailed examination of weld metals has revealed a martensite-austenite microconstituent which can reduce toughness, depending on type, size and location. Garland and Kirkwood[9] found low toughness when the microconstituent existed as large blocky particles of lath martensite associated with bainitic carbides in segregated pools. Toughness was enhanced if the particles were fine, uniformly distributed and in the form of higher carbon twinned martensite.

The objective of the program discussed in this paper was to provide a detailed analysis of the microstructure that can be found in C/Mn and HSLA weld metals as a function of heat input/cooling rate and weld composition. This program was integrated with the ongoing research programs being undertaken in the broad areas of energy production and transportation by Ontario Hydro Research Laboratories, Dominion Bridge Co. Ltd. and Canada Centre for Mineral and Energy Technology, Department of Energy, Mines and Resources.

A. G. GLOVER and J. T. McGRATH are Scientific Officers, Canadian Welding Development Institute; M. J. TINKLER, formerly a graduate student at the University of Toronto, is with Ontario Hydro Research Laboratory, Toronto; and G. C. WEATHERLY is Associate Professor, Department of Metallurgy & Materials Science, University of Toronto, Toronto, Canada.

Experimental Procedure

Weldment Series "A"

A series of single pass, bead on plate weldments was prepared by the submerged arc process in Grades 516 (Nb containing) and 515 pressure vessel steels (analyses in Table 1). A range of weld metal microstructures was produced by varying the heat input from 0.74 to 10 kJ/mm. The cooling rates associated with the weld preparation are included in Table 2.

The weld metal microstructure was analyzed by optical and electron microscopy. For the optical examination a standard 2% nital etchant was used to reveal the ferritic and bainitic constituents. In order to identify the carbon-rich microconstituents a saturated picral etchant was employed.[10] T.E.M. analysis was carried out by standard sectioning and thinning techniques. When a quantitative analysis of microconstituents was required a point counting technique was used. For each weld specimen a total of 1000 counts were made in 10 areas at a magnification of ×2000.

Weldment Series "B"

A two-pass weld was prepared by the standard submerged arc process in 12.5 mm (0.5 in.) thick X70 grade HSLA plate, using the suitable bare electrode and flux, i.e., Linde 44 wire (AWS EF2 electrode) and 166P flux.

The compositions of the plate and weld metal are listed in Table 1. In order to study the effect of cooling rate upon weld metal microstructure, temperature cycling tests were performed, using a Gleeble machine. The Gleeble specimens had a 6.25 mm (¼ in.) diameter and were 50 mm (2 in.) long; they were machined from the center of the second pass of the submerged-arc weld metal.

Table 1—Material Composition, %

Weldment	C	Mn	Si	Mo	Ni	Nb
Series A1:						
A516 base metal	0.18	1.1	0.25	< .01	n.d.	0.035
weld	0.13	1.1	0.25	0.21	n.d.	0.010
Series A2:						
A515 base metal	0.32	0.71	0.20	n.d.	n.d.	n.d.
weld	0.17	1.1	0.30	0.24	n.d.	n.d.
Series B:						
X70 base metal	0.06	1.35	0.63	n.d.	n.d.	0.1
weld	0.07	1.27	0.49	0.18	0.27	0.052

Table 2—Welding Conditions—Series "A" Weldments

Weld	Heat input, kJ/mm	Δt at 800-500 C, s
A1a	0.74	4.4
A1b	1.3	7.3
A1c	2.4	14
A1d	4.3	23
A1e	7.4	39
A2a	10	100

The specimens were rapidly heated, within 10 seconds (s), to an austenitizing temperature of 1350 C (2462 F), then cooled over a range of cooling rates, i.e., Δt 800–500 C = 500, 190, 100, 30 and 15 s. It was felt that rapid heating of the weld metal prior to cooling would ensure that all elements in solution after initial preparation of the weld would remain in solution.

As indicated in the typical heating/cooling cycle in Fig. 1, the time at the maximum austenitizing temperature was approximately 2 s. These Gleeble simulation experiments differ from the cooling of an actual weld from the melt, principally in the size and shape of the austenite grains. The austenite grains in the simulation tests were smaller and polygonal in shape (see Fig. 6 for prior austenite grain size) compared to the elongated, columnar austenite grains in a real weld. The resulting simulated weld microstructures were analyzed by optical and transmission electron microscopy as outlined for Weldment Series "A."

Relationship Between Microstructure and CCT Diagram

Because weld metals are subjected to continuous cooling upon solidification, the resultant microstructures should be predictable from CCT diagrams if they are available for the particular weld metal composition. However, in the majority of instances these diagrams are not readily avail-

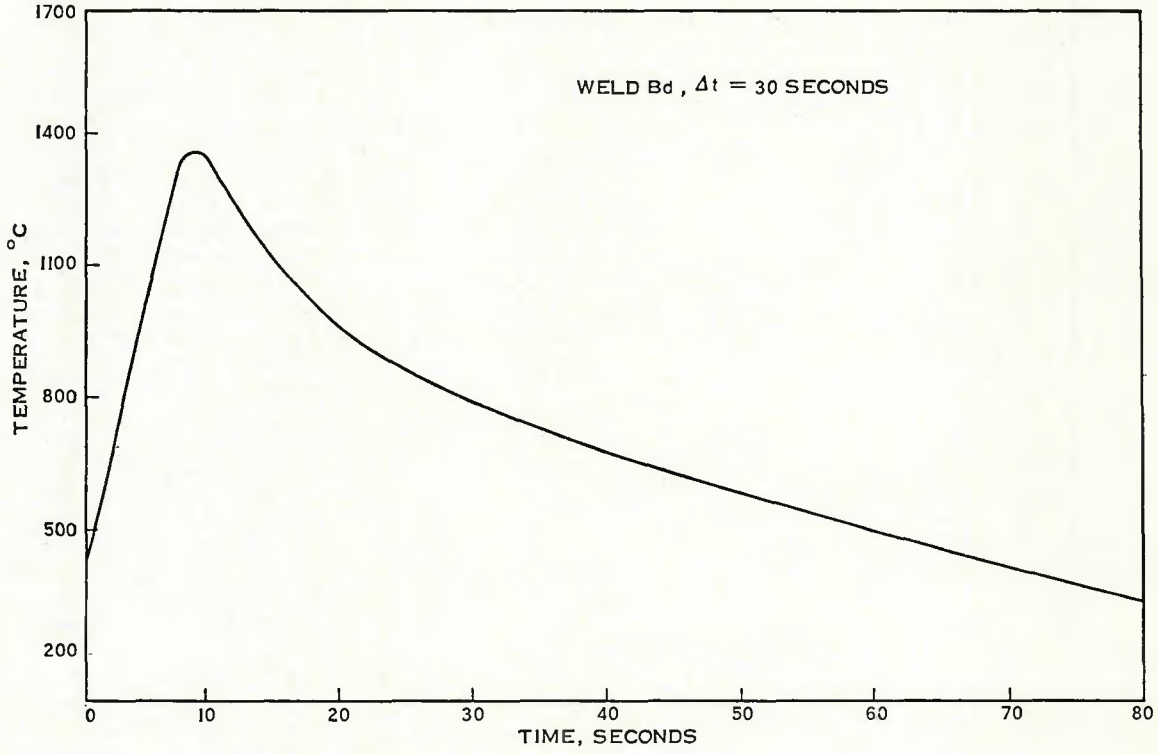

Fig. 1—Heating/cooling cycle during Gleeble simulation

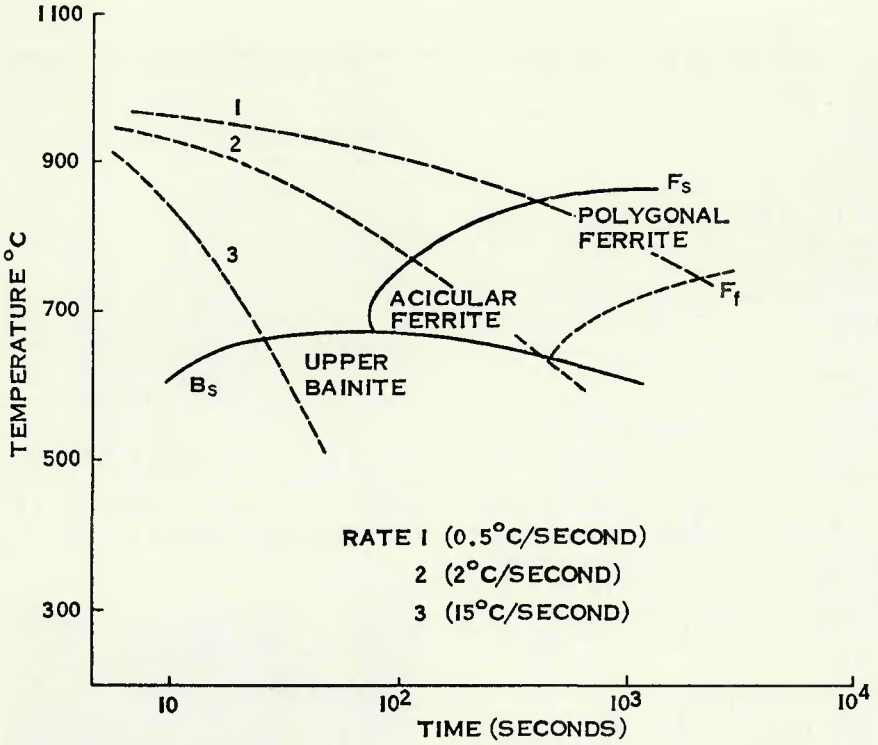

Fig. 2—Schematic CCT diagram

able. Therefore, before presenting the results of the metallographic analysis of the various weld metals, a brief summary of the type of weld metal microstructure that can result as a function of cooling rate is given.

The effects of three cooling rates are considered in the schematic CCT diagram (for a low C steel) of Fig. 2. At the slowest rate, austenite transforms to a coarse polygonal ferrite with regions of pearlite. The amount of pearlite will depend upon the carbon content of the weld metal. At the intermediate rate, coarse ferrite (proeutectoid ferrite) will form initially along austenite grain boundaries. Transformation of the remaining austenite can result in an acicular ferrite structure as the transformation temperature decreases.

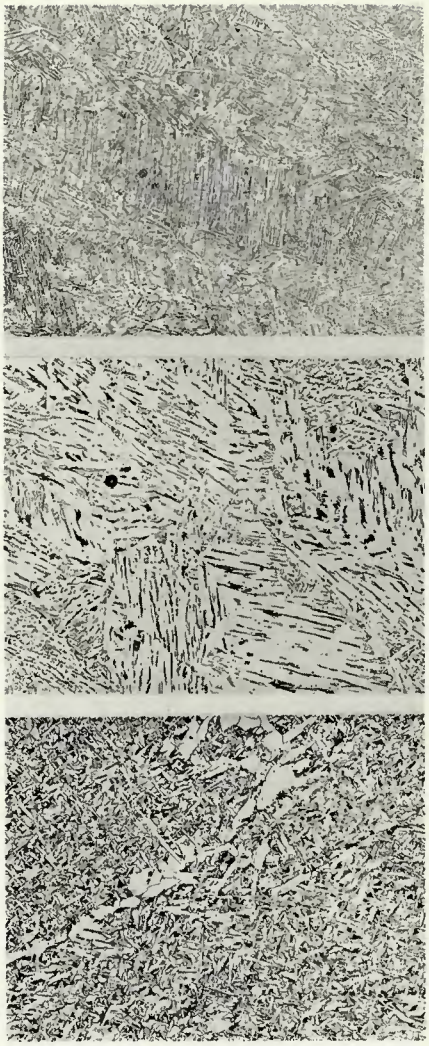

Fig. 3—Micrographs of welds made using 0.74 kJ/mm: A (top)—martensitic structure, weld A1a; B (center)—upper bainite, weld A1e; C (bottom)—acicular ferrite, weld A2a. Nital etch, ×500 (reduced 50% on reproduction)

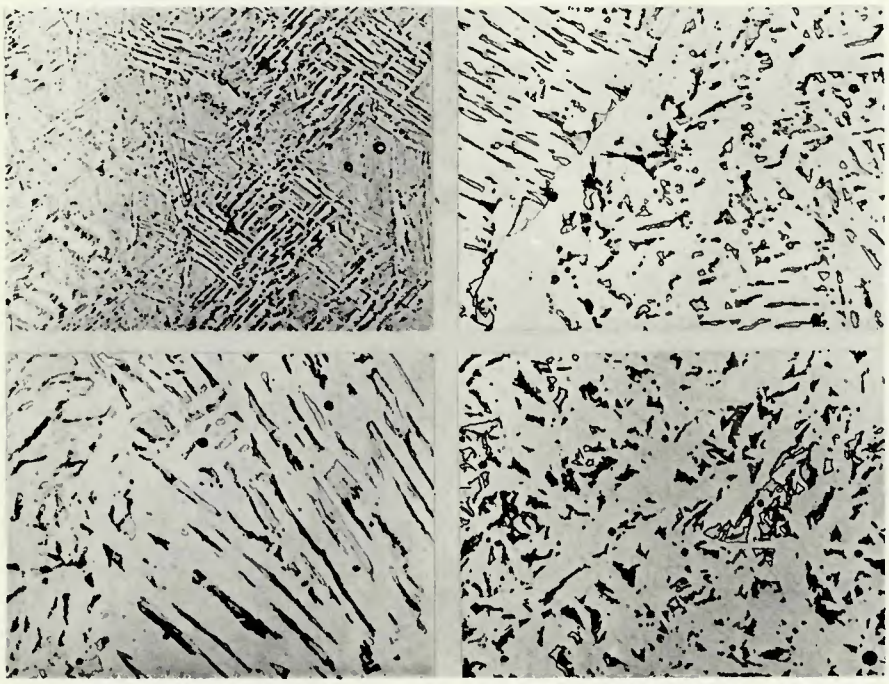

Fig. 4—Micrographs of welds prepared with picral etch: A (top left)—weld A1a, bainite regions with rectangular M-A particles "A" are indicated; B (top right)—weld A1c, dark etching carbides are indicated, and lighter particles are M-A constituent; C (bottom left)—mixture of carbides and M-A particles in weld A1e; D (bottom right)—carbide particles in weld A2a, light particles are M-A. ×2000 (reduced 50% on reproduction)

The formation of acicular ferrite at temperatures above the bainite start temperature has been suggested by other investigators.[11,12] When the weld metal is cooled at the fastest rate, according to Fig. 2, austenite will transform to an upper bainitic structure with no proeutectoid ferrite at prior austenite grain boundaries. The lower the bainite start B_s temperature, the finer will be the grain size of the bainite colonies.

Of emerging importance, particularly in low carbon HSLA steels, are the microconstituents which form in the cooling range that results in the acicular ferrite and bainitic type microstructures. These microconstituents can take the form of carbides or particles of martensite-austenite.[13]

This brief introduction to the influence of cooling rates on microstructure provides a simple framework

for understanding the structures produced in the present study.

Results of Metallographic Analysis

Weldment Series "A"

In the bead on plate welds prepared in the structural steels A516 and A515, the range of heat inputs provided cooling rates which resulted in a spectrum of weld metal microstructures. These ranged from a high martensitic content at the lowest heat input, through upper bainite to an acicular ferrite structure at the highest heat input.

The principal constituent at the low heat input of 0.74 kJ/mm was lath martensite—Fig. 3A. This is essentially a low carbon form of martensite with a maximum hardness of 390 VHN. As shown in Fig. 4A, the picral etch revealed, in addition to martensite, regions of bainite with rectangular shaped particles residing between the bainitic ferrite laths. If any carbides formed at this low heat input, they were very difficult to resolve optically. Quantitative analysis indicated the weld structure to be composed of 61% lath martensite, 8% M-A and 31% bainitic ferrite.

When this structure was examined in the T.E.M., the rectangular particles were always dark (Fig. 5A), which is a characteristic[13] of the M-A constituent discussed earlier. It is shown later that twinning can be observed within the larger M-A particles produced at slower cooling rates. Some fine carbide particles were observed, primarily within the regions of lath martensite.

As the heat input increased, bainite replaced the lath martensitic structure, and as before, elongated M-A particles were observed between the bainitic ferrite laths. At a heat input of 2.4 kJ/mm, carbides that could be clearly resolved in the optical microscope began to form along with the M-A particles.

As shown in Fig. 4B, these carbides appeared as dark particles on etching with picral, while the M-A constituent was only lightly stained with its boundaries clearly delineated. Quantitative analysis indicated that this structure contained 10% M-A and less than 0.3% carbides.

A coarse bainite formed at the heat input of 7.4 kJ/mm (Fig. 3B). The picral etch revealed carbides (6.3 vol-%) as well as M-A (6.2 vol-%) between the bainitic ferrite laths. As shown in Fig. 4C, the M-A was in the form of blocky or elongated particles, with the carbides forming both within the M-A particles and at the M-A ferrite boundaries. The classical concept of upper bainite, i.e., ferrite laths separated by elongated carbides, was noted in the T.E.M. study of the same specimen—Fig. 5B.

At the maximum heat input/slowest cooling rate, proeutectoid ferrite and acicular ferrite, interspersed with agglomerated carbides, were observed as shown in Fig. 3C. Preferential etching with picral revealed that carbon was present predominantly as carbides with only occasional M-A particles (Fig. 4D).

Table 3—Simulated Weld Cooling Conditions—Series "B" Weldments

Weld	Δt at 800-500 C, s
Ba	500
Bb	190
Bc	100
Bd	30
Be	15

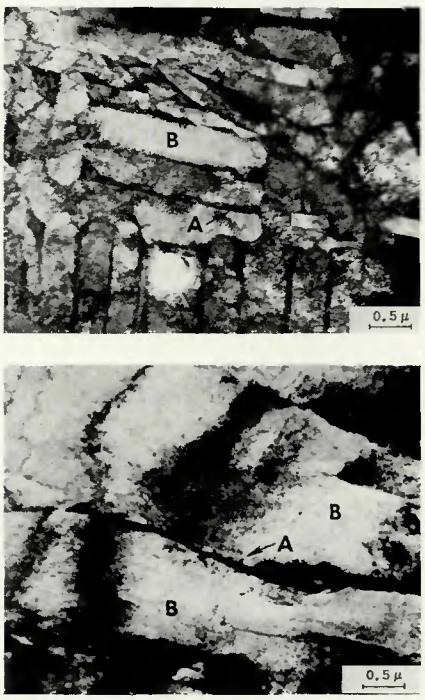

Fig. 5—Examination by transmission electron microscopy (T.E.M.): A (top)—weld A1a with elongated M-A structure A between laths of bainitic ferrite B; B (bottom)—weld A1e with carbides A along boundaries of bainitic ferrite B

Weldment Series "B"

The HSLA weld metal used in the Gleeble simulation experiments differed in composition from the welds in Series "A," principally in its lower carbon and higher niobium contents. The cooling rates, Table 3, provided the variation in microstructure one would expect in welds prepared by the range of heat input conditions used in the submerged arc process.

The nital etchant revealed a coarse polygonal ferrite at the slowest cooling rate, i.e., Δt = 500 s. Because of difficulties in maintaining extended cooling cycles the simulation experiment was interrupted before the transformation was completed. Thus, the amount of pearlite formed could not be determined.

As the cooling rate increased, the austenite transformed initially to proeutectoid ferrite at the austenite grain boundaries (region A in Fig. 6A) with the grain interiors transforming to an acicular ferrite structure at lower transformation temperatures. The amount of proeutectoid ferrite decreased as the cooling rate increased. At a cooling rate of Δt = 30 s, there was very little observable proeutectoid ferrite, with acicular ferrite and regions of upper bainite being detected—Fig. 6C. At the fastest cooling rate, Δt = 15

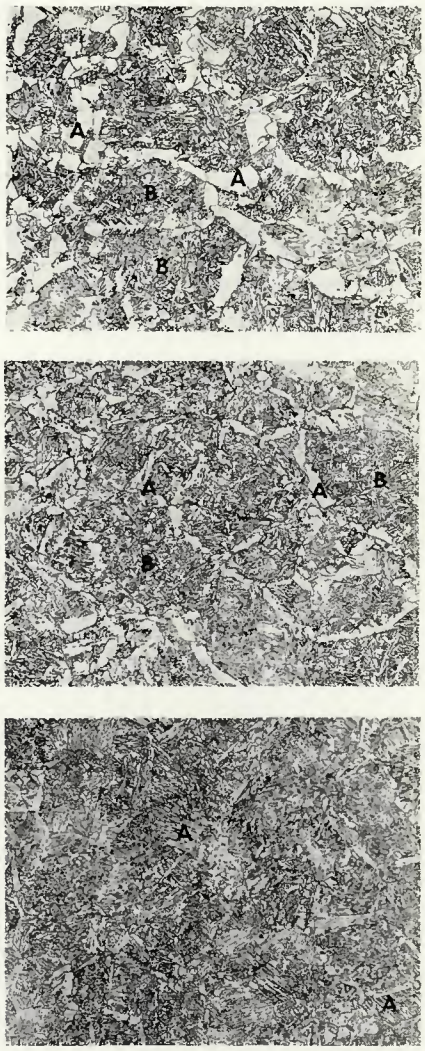

Fig. 6—Micrographs of welds prepared using nital etch: A (top)—weld Bb, cooling rate Δt = 190 s, proeutectoid ferrite A and acicular ferrite B; B (middle)—weld Bc, cooling rate Δt = 100 s, proeutectoid ferrite A and acicular ferrite B; C (bottom)—weld Bd, cooling rate Δt = 30 s, acicular ferrite with regions of coarse bainite A. ×250 (reduced 50% on reproduction)

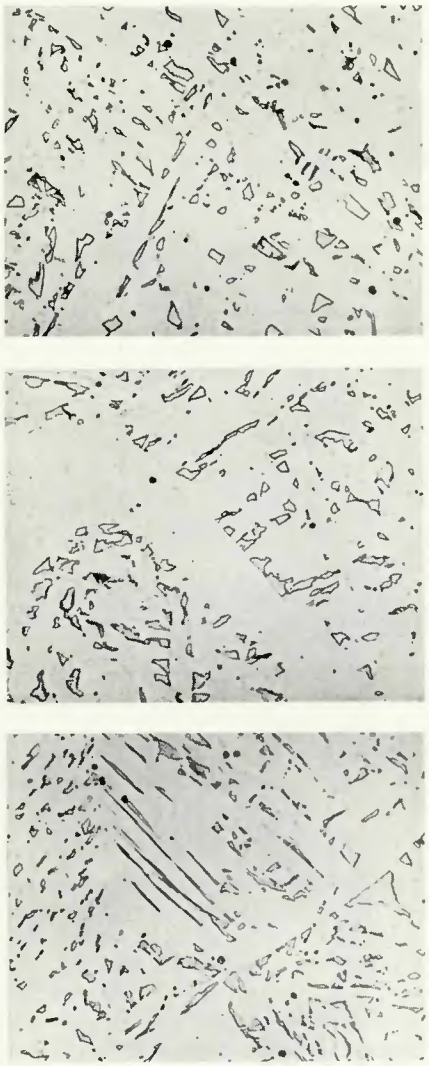

Fig. 7—Micrographs of welds prepared using picral etch: A (top)—weld Bb, showing blocky particles of M-A; B (middle)—weld Bc with blocky M-A particles; C (bottom)—weld Bd with blocky and elongated M-A particles. ×2000 (reduced 50% on reproduction)

s, the structure was predominantly upper bainite.

The picral etchant revealed the carbon-rich regions of the weld metal microstructure. At the intermediate cooling rates (Figs. 7A and 7B) a well-distributed array of blocky particles with no indication of carbide formation was observed among the acicular ferrite. These particles are identical to the martensite-austenite (M-A) microconstituent described by others.[4] At the faster cooling rates, the M-A particles between the laths of bainitic ferrite were elongated, as shown in Fig. 7C. Once again no visible carbides were associated with these M-A particles. The amount of M-A measured by the point counting technique was approximately 10% for all four samples.

Further identification of the M-A particles was done by T.E.M. In Fig. 8A the blocky M-A particles appear as dark areas, with twins being formed within some of the particles. Selected area diffraction of several M-A particles (Fig. 8B) failed to indicate any difference in structure from the surrounding matrix, indicating that the majority of them had transformed from austenite to twinned martensite.

Discussion

It has been shown in this study that the nature and volume fraction of weld metal constituents are dependent upon the heat input (cooling rate) and weld composition in C/Mn and HSLA steels. The formation of the different ferrite constituents (proeutectoid ferrite, acicular ferrite, bainite) or lath martensite can all be rationalized in qualitative terms from the schematic CCT diagram of Fig. 2 and the cooling rates employed—Tables 2 and 3. However, the main objective of this study was to clearly characterize the nature and distribution of the carbon-rich microconstituents, i.e., to determine whether the carbon is present as discrete particles of cementite (or other carbide), or is retained in solid solution as austenite or twinned martensite (the M-A constituent).

This is an important distinction, since the carbon content of a twinned martensite particle may be as low as 0.5% C, whereas cementite contains 6.7% C. Thus, the volume fraction of hard brittle particles would be much greater in the former case with most of the carbon present as martensite-austenite. The impact properties of the M-A containing steel would then be inferior if both Fe_3C and martensite particles acted as equally efficient crack nucleation sites. This deterioration has been demonstrated by Coldren *et al*[14] for a series of low carbon bainitic steels with Mn contents $> 0.8\%$ where the M-A constituent is found. This problem of poor impact properties may be compounded, particularly in welds, by the segregation of M-A or carbides to ferrite boundaries, as clearly shown by Figs. 4 and 7 in this study.

The major findings of the present study are:

1. At a carbon level in the order of 0.13% (Series "A") increasing the continuous cooling rate from $\Delta t = 100$ seconds to $\Delta t = 7$ s results in a change from a fairly uniform blocky carbide distribution (Fig. 4D) to an elongated carbide M-A mixture (Fig. 4C), and finally to a predominantly elongated M-A structure (Fig. 4B). This change in cooling rate also results in an acicular ferrite structure being replaced by upper bainite.

2. At a fixed continuous cooling rate

Fig. 8—Identification of M-A particles by T.E.M: A (top)—weld Bc, with twinned martensite within large M-A particles; B (bottom)—electron diffraction pattern of M-A particles, wherein split spots indicate twinned martensite

(within the range $\Delta t = 100$ to 30 s), decreasing the carbon content of the weld metal promotes the formation of M-A rather than carbide. (There are minor differences in the other alloy contents between Series "A" and "B," but we believe the major difference lies in the carbon content.)

Although many authors have noted the formation of M-A in high Mn, low C steels, only two previous investigations are directly relevant to the present work. Habraken and Economopoulos[13] were the first to clearly establish the importance of continuous cooling rate and isothermal treatment temperatures on M-A formation. Of the various steels they studied, a C/Mn structural steel (#7 in their paper) had a similar composition to the Series "A" welds in our study, although the boron content of their steel (0.0017%) and the higher Mo content (0.45% vs. 0.21%) would alter the position of the ferrite nose and B_s start temperature on the CCT curve.

The CCT diagram for their steel is given in Fig. 9, illustrating the cooling rates utilized in their program. They observed a carbide-ferrite aggregate at a cooling rate of 0.02 C/s. As the cooling rate increased from 1 C/s to 13 C/s, this structure was replaced first by equiaxed and then by elongated M-A particles residing between the bainitic ferrite laths. Our observations (Fig. 4) are in accord with these results.

When transformations took place

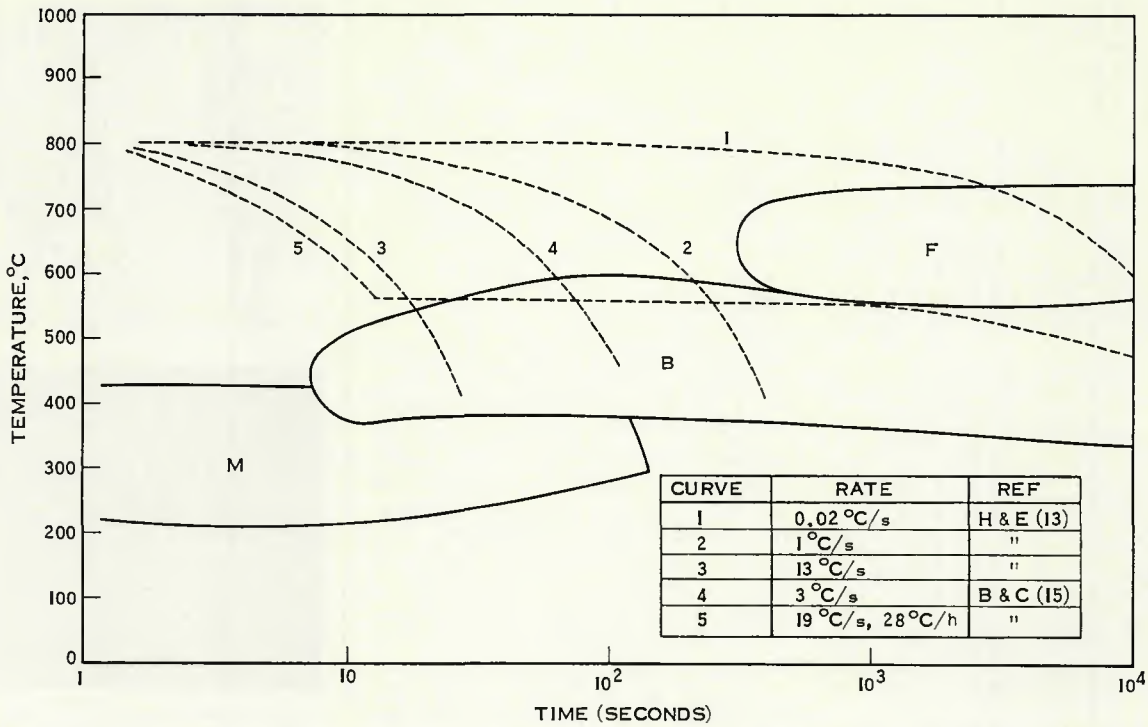

Fig. 9—CCT diagram for a C/Mn/Mo steel indicating range of cooling rates in studies by Habraken and Economopoulos,[13] and Biss and Cryderman[15]

under isothermal conditions, Habraken and Economopoulos indicated that an M-A structure formed only at or near the B_s temperature (550 C in Fig. 9) while further undercooling to 500 C (932 F) gave a bainitic structure with carbides and very little M-A.

The results of Habraken and Economopoulos and our own are at first sight contradicted by those of Biss and Cryderman[15], who suggested that increasing the cooling rate can eliminate the M-A constituent and promote carbide formation instead at ferrite lath boundaries. The steel of composition "A" in the Biss and Cryderman work is comparable to Series "A" in our study and steel #7 in Habraken and Economopoulos' work, although again the boron content of the Biss and Cryderman steel (0.003%) prevents an exact comparison with our own.

The cooling rates employed by Biss and Cryderman are included in Fig. 9. They found the maximum M-A formation in a plate that was spray cooled at 19 C/s to 565 C (1049 F), followed by a programmed cool to 480 C (896 F) at a rate of 28 C/h. This cooling process is not a continuous one in that it involves two steps. The initial cooling reduces the temperature close to the B_s line, with the austenitic structure being maintained. Since the second step in the cooling process is very slow, it is almost akin to the isothermal transformation conditions at 550 C (1022 F) described by Habraken and Economopoulos.

The M-A structure that results from these cooling conditions is in agreement with the observations of Habraken and Economopoulos. On the other hand, when the same steel was continuously air cooled at 3C/s, the resultant microstructure contained a mixture of M-A and carbides which is comparable to that observed in weld "A1e"—Fig. 4C. This cooling rate is in the middle of the range of those studied by Habraken and Economopoulos (see Fig. 9) and a mixed microstructure would be expected.

The special cooling conditions used in Biss and Cryderman's study attempted to simulate those found in the production of hot rolled strip. However, the results of their study cannot be extended to the much faster cooling rates characteristic of the submerged arc welding process.

In this range of cooling rates (from 1 C/s to 41 C/s), where the ferrite structure is either acicular or upper bainite laths, both our study and that of Habraken and Economopoulos have shown that M-A formation is favored as the cooling rate is increased. At the very fastest cooling rate (weld "A1a"), the microstructure is a mixture of very fine bainite and lath martensite—Fig. 4A. The scale of the structure is clearly much finer in this weld; this, together with the shear nature of the transformation at these cooling rates makes any comparison with the carbon distribution at slower cooling rates rather meaningless.

The influence of cooling rate and composition on the formation of M-A or carbides can be explained by considering the driving force available for carbide nucleation. Transformation close to the B_s line in Fig. 9 produces ferrite laths, but the build-up of carbon in the untransformed austenite is apparently insufficient to provide enough carbon supersaturation for carbide nucleation. On cooling, the carbon-enriched austenite is either retained or transforms to twinned martensite at a temperature which, for these steels, is adequately predicted by the Steven and Haynes formula:[16]

$$M_s \simeq 521\text{-}474\ (\text{wt-}\%C)\ °C$$

where the wt-%C value would be that of the locally enriched austenite composition.

In using Steven and Haynes' formula, we have assumed that only segregation of carbon takes place, the other alloying elements having the same composition as the bulk. This assumption is supported by the work of Biss and Cryderman. The amount of M-A found in this and other studies ranges from 8 to 20%; if there is no carbide formation and little carbon in solution in the ferrite, the local carbon content in the austenite could vary in the range of 1-2% for a steel of nominal 0.15-0.2% C composition.[15]

Isothermal transformation at lower temperatures (500 C—Fig. 9) or continuous cooling at intermediate rates (1-10 C/s—Fig. 9) provides sufficient driving force for carbide nucleation. One can consider this increased driving force to come from both the ther-

modynamic supercooling effect associated with the austenite to carbide transformation and the size of the carbon "spike" that builds up in the austenite ahead of a growing ferrite lath, as outlined by Biss and Cryderman.

At faster cooling rates (> 20 C/s for the Series "A" welds in this study) bainitic ferrite laths still form, but there is now insufficient time for carbides to form and M-A is again predominantly the final transformation product of the carbon enriched austenite. Carbide formation in this temperature range apparently follows the normal "C-curve" kinetics found in nucleation and growth transformations.

The influence of carbon on the propensity to form either M-A or carbides is clearly demonstrated in this work. The structures of the two weld series "A" and "B" can be compared at the same cooling rates, $\Delta t = 30$ or 100 s. As shown in Figs. 3C and 6B, the gross microstructures of welds "A2a" and "Bc" are comparable (apart from the austenite grain size effect mentioned earlier), suggesting that the ferrite nucleation characteristics are similar in the two alloys and are not affected by carbon content. However, the carbon containing microconstituents are very different, the low carbon weld "Bc" having blocky M-A particles with no carbides, while carbides with very little M-A formed in weld "A2a." The same trend was found at the faster cooling rate, with blocky and elongated M-A in the low carbon "Bd" weld, and a mixture of M-A and carbides in weld "A1e."

Lowering the carbon level in the untransformed austenite raises the local M_s temperature (about 50 C for each 0.1 wt-% C) and decreases the available carbon supersaturation for carbide nucleation—both factors promoting M-A rather than carbide formation. An estimate of the local carbon level in austenite necessary for carbide formation can be made from the data presented earlier. The M-A content in weld series "B" was approximately 10% for all four cooling rates.

If the carbon level of the surrounding ferrite is assumed to be 0.01%, the amount of carbon in M-A would be 0.6%, a level too low apparently for carbide nucleation. On the other hand, for specimen "A1c," with an average carbon level of 0.13% and a measured M-A content of 10%, the M-A should contain 1.2% carbon (assuming the ferrite again contains 0.01% C), and carbide nucleation is now possible as observed.

Conclusions

The weld metal microstructure for a series of weldments prepared in C/Mn and HSLA steels can be summarized as a function of heat input/cooling rate and composition:

1. The gross microstructure of weld metals with a carbon content of $\geq 0.13\%$ was found to change from martensite to upper bainite to acicular ferrite as the heat input was increased in the range 0.74 to 10 kJ/mm. An M-A microconstituent, residing between the ferrite laths, was replaced by carbides with increasing heat input (slower cooling rate).

2. For the lower carbon (C = 0.07%) HSLA weld metal, increasing the cooling rate, $\Delta t = 500 \rightarrow 15$ seconds (s), resulted in the gross microstructure changing from coarse, polygonal ferrite to acicular ferrite to upper bainite. In the cooling range, $15 < \Delta t < 190$s, a blocky or elongated M-A microconstituent was observed. The absence of any distinct carbide formation in this cooling range was noted.

Acknowledgements

The authors wish to thank Mr. I.D. Montgomery for his technical expertise in all phases of the metallographic analysis. They also wish to thank Ontario Hydro Research Laboratories for the use of experimental facilities, Dr. J. Gordine, CANMET, Department of Energy, Mines and Resources, for carrying out the weld simulations, and Mr. B. Graville, Dominion Bridge Company Ltd., for supplying the Series A_1 weldments. One of the authors, M.J. Tinkler, acknowledges the financial assistance of a National Research Council fellowship.

References

1. Bibby, M.J., and Rothwell, A.B., "The Welding of High Strength Low Alloy Pipeline Steels," Noranda Research Centre, Pointe Claire, Quebec, Tech. Mem., No. 37, Feb. 1975.

2. Tichaurer, P.A., "The Submerged Arc Weld in HSLA Pipe—A State of the Art Review," WRC Bulletin 201, Dec. 1974.

3. Cordea, J.N., "Niobium and Vanadium Containing Steels for Pressure Vessel Service," WRC Bulletin 203, Feb. 1975.

4. Levine, E., and Hill, D.C., "A Review of the Structure and Properties of Welds in Columbium or Vanadium Containing High Strength Low Alloy Steels," WRC Bulletin 213, Feb. 1976.

5. Farrar, R.A., Tuliani, S.S., and Norman, S.R., "Relationship Between Fracture Toughness and Microstructure of Mild Steel Submerged Arc Weld Metal," *Weld. and Met. Fab.*, Feb. 1974, pp. 68-73.

6. Taylor, L.G., and Farrar, R.A., "Metallurgical Aspects of the Mechanical Properties of Submerged Arc Weld Metal," *Weld. and Met. Fab.*, May 1975, pp. 305-310.

7. Glover, A.G., McGrath, J.T., and Eaton, N.F., "The Control of Fracture Toughness in Structural Steel Weldments," *Proc. of Conf. Materials Engineering in the Arctic*, Gray Rocks, Quebec, 1976, to be published.

8. Widgery, D.J., "Deoxidation Practice for Mild Steel Weld Metal," *Welding Journal*, Vol. 55 (3), March 1976, Res. Suppl., pp. 57-s to 68-s.

9. Garland, J.G., and Kirkwood, P.R., "The Notch Toughness of Submerged Arc Weld Metal in Micro Alloyed Structural Steels," Brit. Steel Corp. Rep., GS/PROD/499/1/74.

10. "Standard Methods of Preparation of Metallographic Specimens," ASTM Std. E3-62.

11. Smith, Y.E., Coldren, A.P., and Cryderman, R.L., "Mn-Mo-Nb Acicular Ferrite Steels with High Strength and Toughness," Sym. Toward Improved Ductility and Toughness, Kyoto, Japan, 1971, p. 119.

12. Boyd, J.D., "The Microstructure and Properties of a Quenched and Tempered Low-Carbon Manganese, Niobium Steel," *Met. Trans. A.*, Vol. 7a, Oct. 1976, p. 1577.

13. Habraken, L.J., and Economopoulos, M., "Bainitic Microstructures in Low-Carbon Alloy Steels and Their Mechanical Properties," Sym. Transformation and Hardenability in Steels, Climax Moly. Co., 1967.

14. Coldren, A.P., Cryderman, R.L., and Semchyshen, M., "Strength and Impact Properties of Low Carbon Structural Steels Containing Molybdenum," Sym. Steel Strengthening Mechanisms, Climax Moly. Co., 1969.

15. Biss, V., and Cryderman, R.L., "Martensite and Retained Austenite in Hot-Rolled, Low-Carbon Bainitic Steels," *Metallurgical Transactions*, Vol. 2, Aug. 1971, p. 2267.

16. Steven, W., and Haynes, A.G., "Temperature of Formation of Martensite and Bainite in Some Low Alloy Steels," *J. Iron Steel Inst.*, Vol. 183, 1956, p. 349.